DOI: 10.13009/EUCASS2019-345

Interface Designs between TPS and Cryogenic Propellant Tank of an RLV Booster Stage

Thomas Reimer Carolin Rauh*Martin Sippel***
**DLR Institute of Structures and Design*
Pfaffenwaldring 38-40, 70569 Stuttgart, Germany
Thomas.Reimer@dlr.de
***DLR Institute of Space Systems*
Robert-Hooke-Straße 7, 28359 Bremen, Germany
Martin.Sippel@dlr.de

Abstract

The booster of the SpaceLiner 7 was chosen as reference vehicle to investigate the design of an integrated system comprising the cryogenic fuel tank with added thermal insulation and a thermal protection system. One solution is a stack of two layers of cryogenic respectively high-temperature insulation adding up to 130 mm. Another option is a purge gap to reduce thickness. Thermal analyses show that the purge gap is feasible on a cryogenic insulation with reduced thickness. FEM analyses show that requirements can be satisfied. A design suggestion was made for the structural fixation of the TPS to the underlying tank.

1. Introduction

Re-usable launch vehicles promise to reduce the launch cost considerably, which has been proven to a certain extent in recent years by the advent of the vertical-take-off/vertical-landing rockets of SpaceX. In DLR there have been system investigations going on about the concept of the SpaceLiner as one kind of a possible future RLV. This two-stage vehicle is envisaged as a vertical take-off and horizontal-landing concept and thus features wings on both of its stages.

In the course of the project AKIRA [1], a number of critical technologies were investigated which are deemed essential to advance the technology of re-usable winged launchers based on liquid-fuel propulsion. The booster stage was looked at in detail to investigate the issue of the overall system consisting of tank, insulation and TPS. Special attention was given to the interfaces between the TPS and the booster structure which is at the same time the integral tank of the vehicle and is covered by cryogenic insulation.

The design challenge arises due to the combination of the super-cold tank and its cryogenic insulation with the TPS that relies on a fibrous, open-pore, high-temperature insulation. Typical cryogenic insulations of closed-cell foams are usually limited to around 100°C in use temperature. On the other hand, fibrous high-temperature insulations should be kept above the dew point of air during ground operations to prevent internal moisture condensation or even icing. Thus, the design objectives are challenging to achieve in one design. For one, the tank shall be insulated as good as possible to keep the fuel at low temperature and prevent fuel loss from evaporation calling for an ideal layer of cryogenic insulation. On the other hand, a TPS is required to protect the structure and insulation from re-entry heat loads. The baseline design chosen for the TPS was to attach rigid surface panels to the underlying structure via dedicated structure fixations penetrating through the insulation, thus disturbing the temperature field in the cryogenic insulation.

Requirements were identified that drive the design. Temperatures inside the high-temperature insulation of the TPS shall not go below the dew point during pre-launch of the vehicle when the tank is loaded with fuel to avoid condensation and icing. The cryogenic insulation was assumed to be a low-density foam, Rohacell, for which an upper limit temperature of 100° C was set.

A baseline insulation system without structure fixations was designed consisting of two layers total of cryogenic and high-temperature insulation based on steady-state conditions of pre-launch plus the following re-entry loads. The baseline layup was calculated for both the position on the hydrogen and the oxygen tank of the booster. The total

DOI: 10.13009/EUCASS2019-345

thickness was quite similar for both cases with approximately 120 mm in total – due to lower heat load on the hydrogen tank but lower fuel temperature.
In addition the concept of a purge gap was considered in order to reduce the total thickness of the insulation system. Via introducing a gap between cryogenic and TPS-insulation through which dry gas at a controlled temperature is fed, the temperature on the cold side of the TPS can be controlled and the effect of condensation or ice-build-up in the insulation can be prevented, while at the same time the thickness of the cryogenic insulation can be reduced. Going from there, concepts were developed for structure fixations that run through both of the insulation layers. In these concepts different types of fixation were looked at and a range of possible material choices were considered, adapted to the individual position of the items. In addition it was investigated how the fixation components could be combined with the design of a purge gap in terms of attachment points of gas feed lines for example.

2. Reference Vehicle

The SpaceLiner 7 was chosen as the reference vehicle [2]. It is designed as a two-stage vehicle with booster stage and orbital vehicle. Both stages are winged, shall be fully re-usable and use rocket motors with liquid-fuel propellant. The propellant shall be liquid hydrogen and oxygen. Since the stages shall be re-usable, they will need a thermal protection system for the re-entry leg of the flight. Separation Mach number is around 12. Figure 1 shows an artist´s view of the SpaceLiner during separation between booster and orbiter. The booster is conceived with a considerable length of 80 m and a wingspan of 36 m. The diameter of the fuselage is 8.6 m. It contains two liquid-fuel tanks. In the front section of the fuselage, the oxygen tank is located with a length of 13 m, the mid and aft section contain the hydrogen tank of 42 m length, depicted in Figure 2.

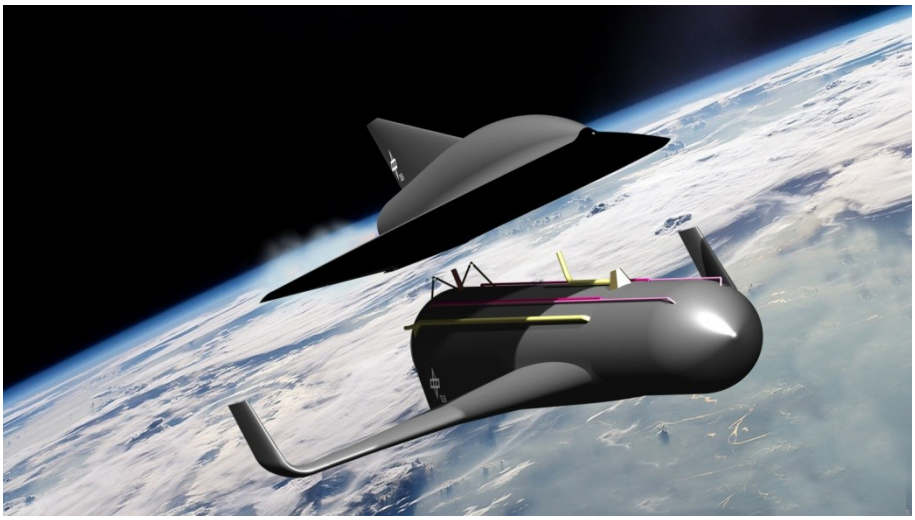

Figure 1: SpaceLiner 7 as artists concept at separation between booster and orbiter.

DOI: 10.13009/EUCASS2019-345

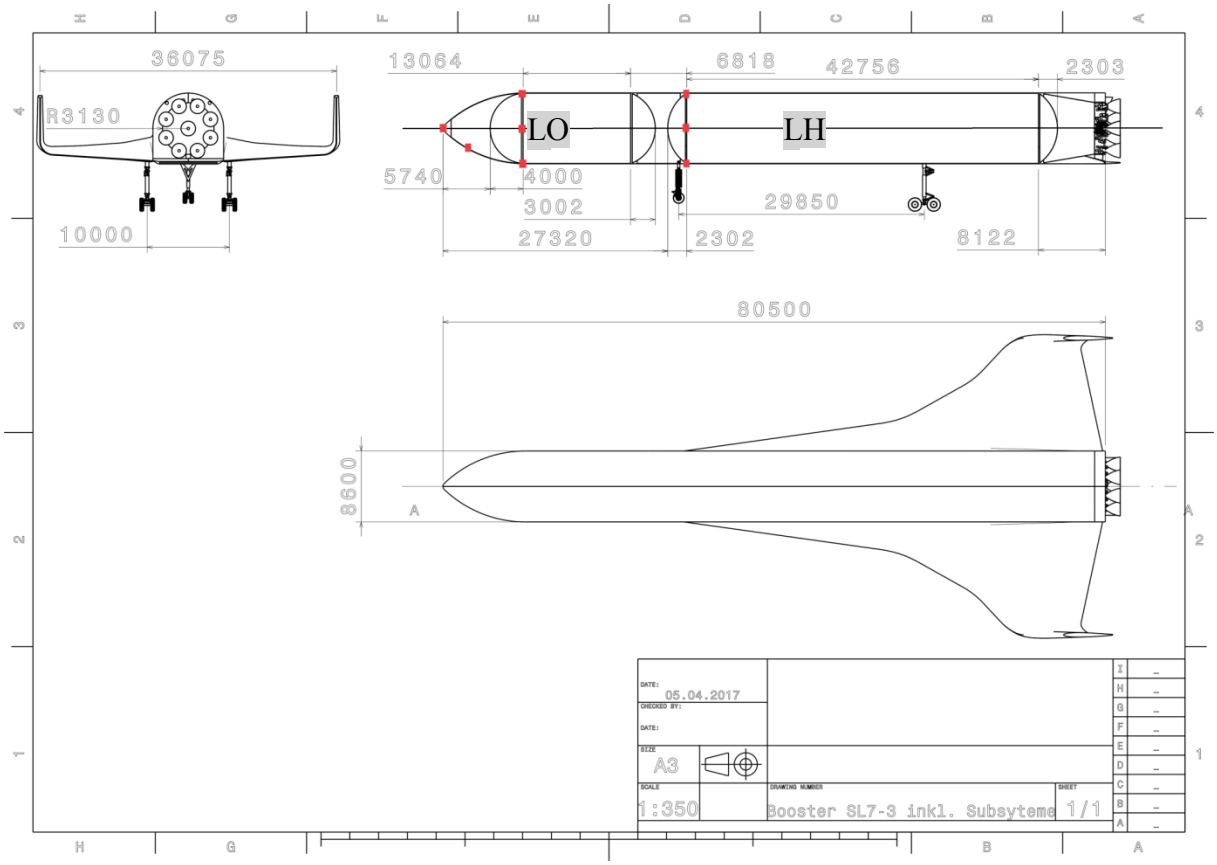

Figure 2: SpaceLiner 7 booster layout.

The concept of the SpaceLiner has been analyzed for some time already. Trajectories with aerodynamic data as well as thermal loads for ascent and re-entry are available. The thermal loads for the design analyses were taken from the trajectory of the booster asenct and re-entry flight. Since the thermal loads vary widely over the surface of the vehicle and over time, a number of characteristic design points were identified for which the loads were extracted from the vehicle data set. The specific locations are given in Table 1 and shown in Figure 2 as indicated via red dots.

Table 1: Design points on the SpaceLiner 7 booster for thermal load determination.

Design Point	Location on vehicle
P0	Nose tip
P1	Stagnation point
P2	Windward side oxygen tank forward
P3	Side oxygen tank forward
P4	Leeward side oxygen tank forward
P5	Windward side hydrogen tank forward
P6	Side hydrogen tank forward
P7	Leeward side hydrogen tank forward

DOI: 10.13009/EUCASS2019-345

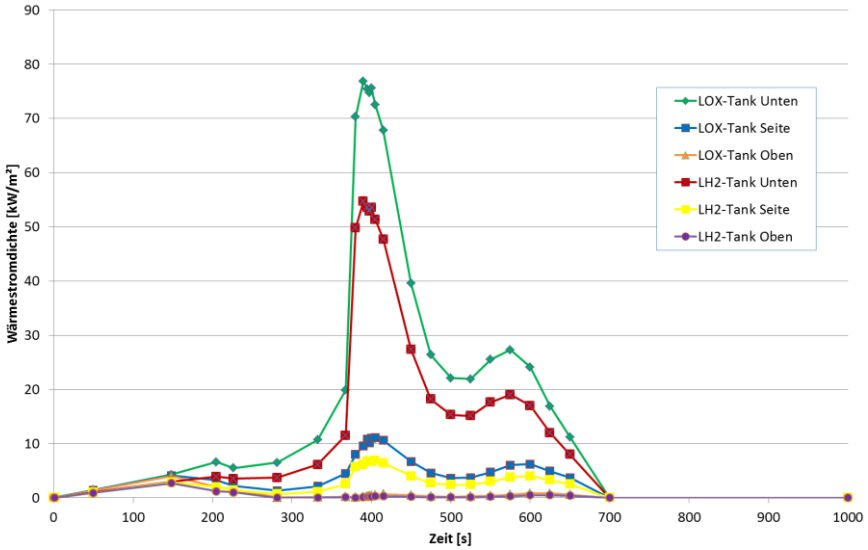

Figure 3: Thermal re-entry loads for selected design points on the SL7 booster.

Figure 3 shows the respective time-dependent heat flux densities of the design points P2-P7. It can be noted that the thermal loads are not very high with peak values around 75 kW/m² for the oxygen tank windward side.

3. Initial Insulation Configuration

As a starting point, 1-D thermal analyses were carried out to investigate possible scenarios of a simplified tank-TPS-configuration. From earlier system work it was a given that the tank is considered a classic aluminum tank with internal stiffening. It was assumed that the cryogenic tank is covered with a dedicated cryogenic insulation, optimized for low-temperature performance and produced from a closed-cell foam. On top of that, a TPS was assumed, consisting of a layer of high-temperature insulation and surface panels made from CMC material.
In terms of the materials considered, the cryogenic insulation was assumed to be Rohacell 51.
The TPS insulation was assumed to be AltraMat 80, a fibrous insulation consisting mostly of Al2O3 and SiO2 fibres.
The CMC panels are C/C-SiC, a material which is produced in-house at DLR Stuttgart. Data of the different materials is given in Table 2.

Table 2: Basic material properties in the temperature range relevant for the simulations.

Material	Density	Capacitance	conductivity	Emittance
	Kg/m³	J/kgK	W/mK	-
Aluminium	2770	875	114 – 175	-
Rohacell 51	51,1	1200 – 2400	0.005 – 0.036	0.5
AltraMat	120	1000	0.038 – 0.086	0.5
C/C-SiC	1900	750 – 1400	16.8 – 18.8	0.8

Uniform layers of aluminum, Rohacell, Altramat and C/C-SiC were considered for the 1-D analyses. Two subsequent load cases were investigated:

- LC1 – tank filling on the launch pad
- LC2 – launch, ascent and re-entry.

The tank filling load case was considered to be a steady-state condition. The filling requires a couple of hours and once a non-negligible amount of liquid propellant is inside the tank, the aluminum tank can be considered to be on the fuel/oxidizer temperature, making this the internal boundary condition. On the outside of the tank, ambient conditions are present and it is important to consider convective heat exchange. As ambient environment, 20° C were assumed. The vehicle is standing upright, so convective heat transfer between a vertical cylinder and the environment was assumed. The heat transfer coefficient is calculated along the VDI Wärmeatlas [3].
Two requirements were set up to guide the analyses:

DOI: 10.13009/EUCASS2019-345

- R1 – minimum temperature of 0°C for the TPS insulation during tank filling.
- R2 – maximum use temperature of 100°C for Rohacell 51.

The analyses were carried out in such a way that, first LC1 was analyzed as the steady-state condition on the launch pad, with the result being the input starting condition for LC2 with the following transient analysis covering ascent and re-entry. To illustrate the process and to demonstrate how the two insulation layers influence each other due to the requirements R1 and R2, an initial configuration with only one layer of 30 mm of Rohacell is considered in the location P5 at the windward side of the forward hydrogen tank.

Steady-state analysis results are shown in the temperature profile in Figure 4. The outside temperature on the CMC panels is very much driven by the ambient temperature, due to the small thickness of the Rohacell, it is a little lower than ambient at 1° C. Due to the slightly temperature-dependent properties of the Rohacell, the temperature profile is also slightly non-linear. Now it is obvious that the Rohacell does need to be protected by a layer of TPS. If a thin layer of 15 mm TPS is added, the line blue line is the result. The important point is the interface between both insulations. In steady-state on the ground, the surface is again close to ambient temperature, this time somewhat warmer at 5° C due to the larger total insulation thickness. This leaves the interface between Rohacell and TPS at approximately -30° C, which is below R1. The other consideration is that R2 has to be satisfied. Doing so and iteratively increasing the TPS leads to a thickness of 27 mm for the TPS to satisfy R2 with the given 30 mm Rohacell, which in turn reduces the interface temperature between Rohacell and TPS even more. The consequence is that the thickness of the cryogenic insulation needs to be increased in turn to check on R1, and then the TPS thickness needs to be increased to check on R2. The whole process finally leads to a solution which satisfies both R1 and R2. In the case of the LH2 tank at P2 the thickness of the cryogenic insulation is 105 mm and the corresponding thickness of the TPS is 13 mm. In the case of the LOX tank the respective values are 105 mm and 16 mm.

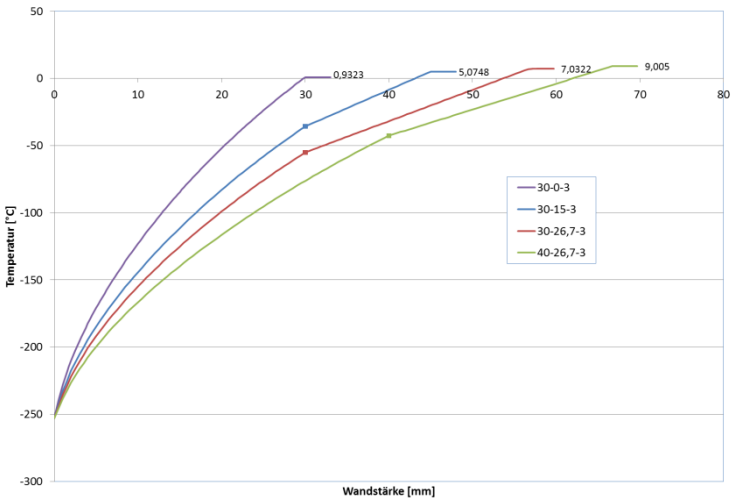

Figure 4: Steady-state temperature profiles.

Table 3: Insulation thickness at desing points P2 and P5 resulting from combined cases LC1 and LC2.

Design Point	Tank	Cryogenic Insulation	TPS Insulation	Total Insulation Thickness
		mm	mm	mm
P2	LOX	105	16	121
P5	LH2	105	13	118

These are rather high values. The system engineering department did not like it a lot. Therefore, it was discussed whether there is an alternative which can shave off some of the insulation thickness.

DOI: 10.13009/EUCASS2019-345

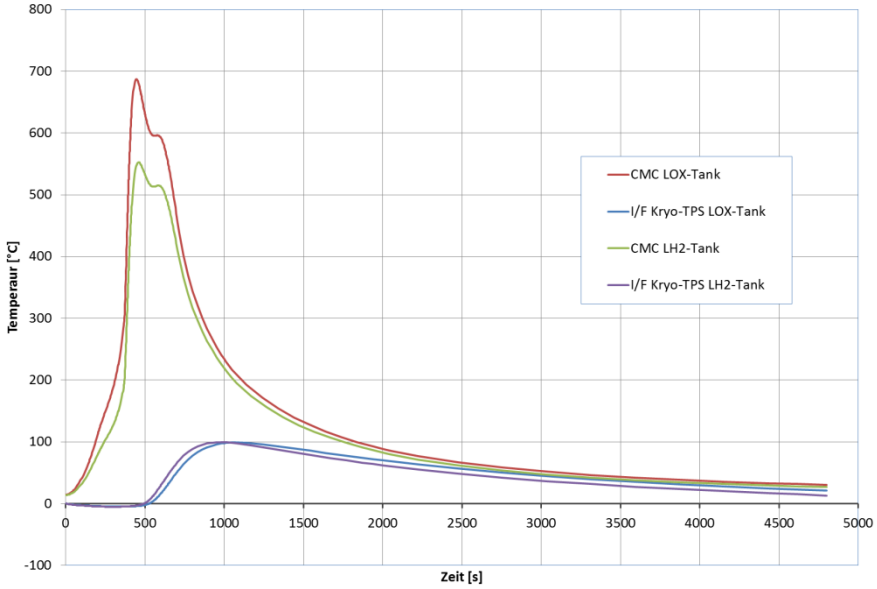

Figure 5: Transient temperatures of surface and insulation IF for P1 and P2.

4. Purge Gap Concept

As a result of the aforementioned considerations, the concept of a purge gap was proposed for analysis. The purge gap is a dedicated hollow space between cryogenic insulation and TPS insulation that is used as a channel to feed dry gas at a controlled temperature between the insulations. The flow is used to transport energy into the system and thus control the interface temperature between the cryogenic and high-temperature insulation. The concept has been investigated before [4].

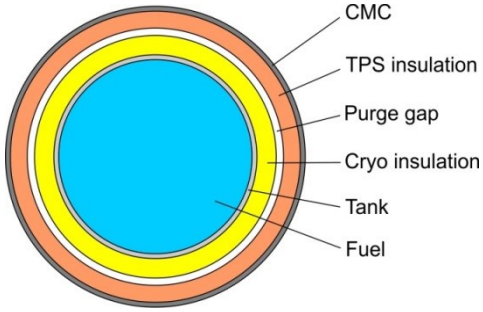

Figure 6: Schematic of the purge gap concept.

To get a grip on it, at first, an analytical approach was used which is employed in heat-exchanger design [3]. The booster fuselage is considered a double-tube heat exchanger with higher temperature on the outside and low temperature on the inside. To further simplify the situation, the outward face of the purge gap was assumed adiabatic. This seemed justified, as the temperature difference over the TPS during tank filling on the ground is only about 20 degrees Celsius, whereas most of the energy is going inside the cryogenic insulation and thus into the tank and fuel.

DOI: 10.13009/EUCASS2019-345

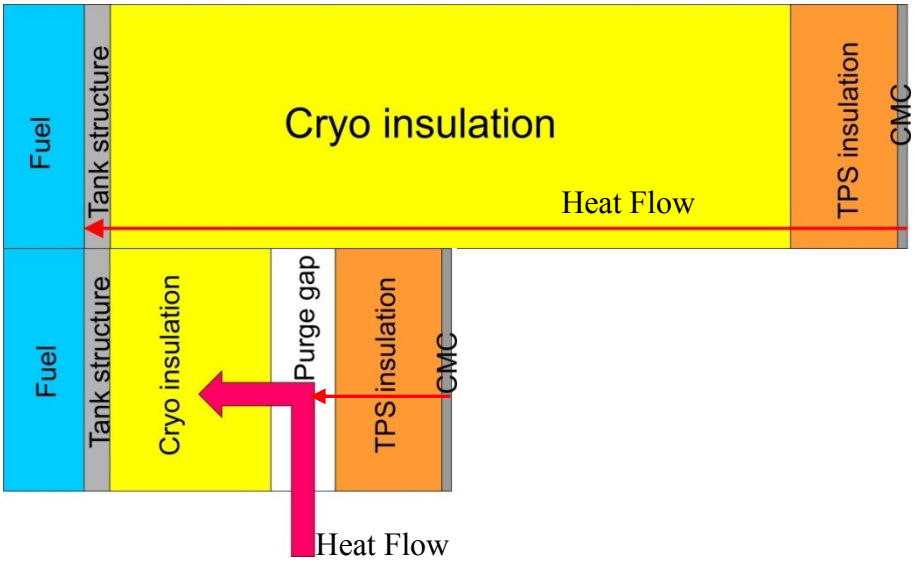

Figure 7: Schematic of the effect of a purge gap on wall thickness and heat flow.

The analytical approach employed here, gives a length as the result. This is due to the fact that it is meant to design heat exchangers. The gas temperature at the circular gap entry is given and also the exit temperature is fixed. Then, also the inner wall temperature is fixed. The analysis procedure varies the length of the gas flow until the boundary conditions are satisfied. The gas velocity is also fixed, the gas properties are calculated depending on pressure and temperature.

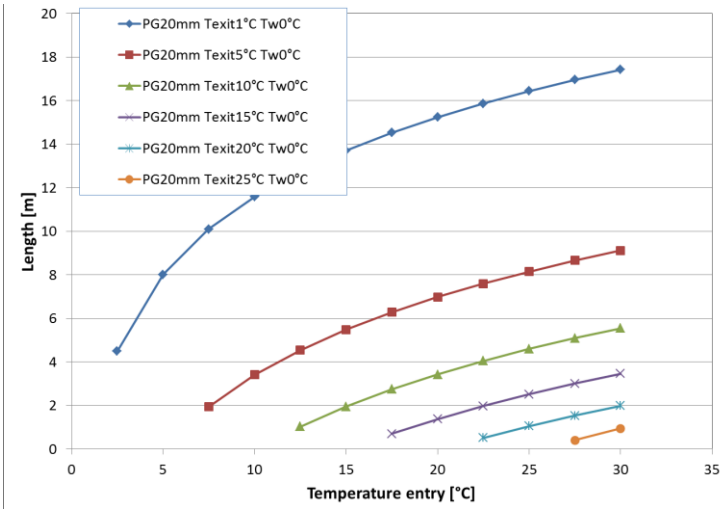

Figure 8: Corresponding gas flow distance for given flow parameters in purge gap. Gas velocity 1 m/s.

Another result from the analytical calculations was the total energy balance for the given conditions. The analysis procedure yields the energy which is required to keep all the parameters in balance. The result was of interest, to assess the feasibility of a purge gap system with respect to the absolute amounts of heat required. Figure 9 shows graphs of the heat flux density plotted over the gas inlet temperature in dependence of gap height and gas velocity. For the parameter values investigated here, the resulting fluxes are on the order of between 50 and 230 W/m². If a maximum value of 230 W/m² is applied on the whole surface of e.g. the oxygen tank with a surface area of 340 m², the resulting heat flow amounts to 78.2 kW which would be necessary to be supplied by ground infrastructure.

DOI: 10.13009/EUCASS2019-345

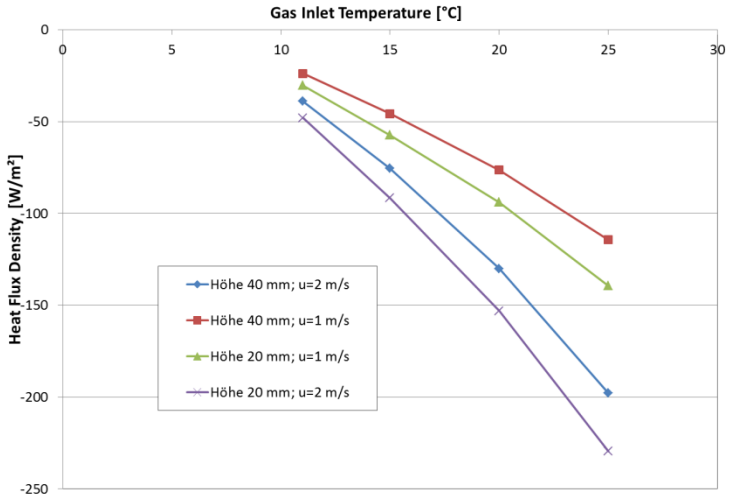

Figure 9: Heat flux density on purge gap inner wall for various conditions.

Another calculation can be made with regard to the thickness of the cryogenic insulation. Since the wall temperature on the inner purge gap wall and also the fuel temperature are given, with the heat flux value as the result of the above mentioned analysis, the thickness of the cryogenic insulation can be estimated which goes along with the purge gap data.

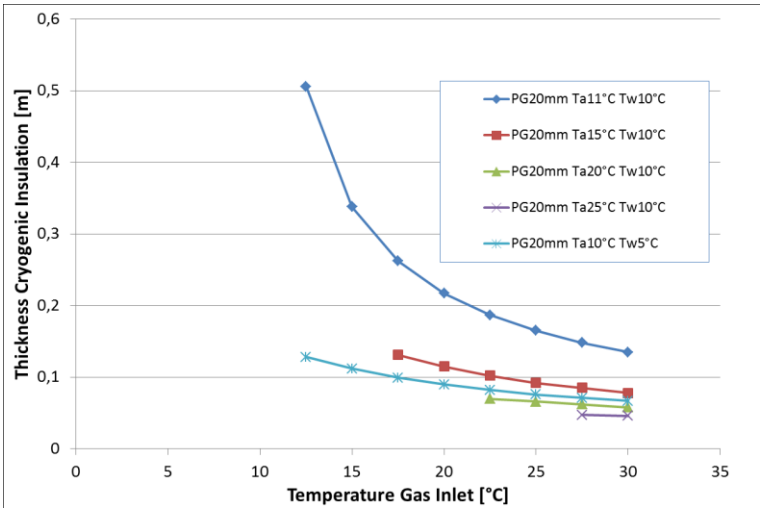

Figure 10: Thickness of the cryogenic insulation corresponding to purge gap data.

From Figure 10 it can be seen that e.g. in the case of a 20 mm purge gap with gas inlet temperature of 20° C, exit temperature 11° C and an inner purge gap wall temperature of 10° C, the corresponding thickness of the cryogenic insulation would be quite high at around 0.217 mm. However, if the gas temperature is increased, to 30° C and exit temperature still 20° C at the same wall temperature of 10° C, the thickness is reduced considerably to 0.067 m. Analysis-wise, the gas exit temperature drives the result, but in reality it is of course the reduced insulation wall thickness that sucks more energy inside and thus needs the gas to contain more heat.
To sum up the exercise on the purge gap, it showed that it should be possible to design a purge gap system and come up with feasible values for gas temperatures, mass and volume flows.

5. Thermal Protection System Design Aspects

Based on the results of the 1-D analysis without any fixation elements and the findings from the analytical purge gap considerations, a model was set up for the purpose of combining the effects of a purge gap with structural fixation elements going right through all the insulation layers. From 2-D simulations which are not presented in detail here, it became evident that in a fixation element connecting surface panel and tank with each other, the type of material with regard to its thermal conductivity is very important and also the order of putting different elements from different materials together. In addition, it became also clear, that there would need to be some kind of active heating

DOI: 10.13009/EUCASS2019-345

of the fixation elements during the tank filling phase before launch to prevent the low temperatures from spreading out into the TPS through the fixation elements.
In order to be able to determine the effects of changes of different materials easily, the model was simplified considerably with respect to the geometry. The fixation element was modelled as a very simple straight connection between tank and surface panel with rectangular cross section.
From the analytical purge gap calculations, it seemed feasible to realize a cryogenic insulation wall thickness of only 30mm. So this was taken as the basis of the model and was not changed in the course of the simulations. Moreover, also the thickness of the TPS insulation was held constant at 15 mm. So the goal of these simulations was really to see if under these boundary conditions the temperature requirements R1 and R2 could be satisfied in the presence of a structural connection between TPS panel and fuel tank by choosing the right materials in the right order for the individual components and by applying some assumedly realistic values for convective heating in the purge gap and at the fixation itself.

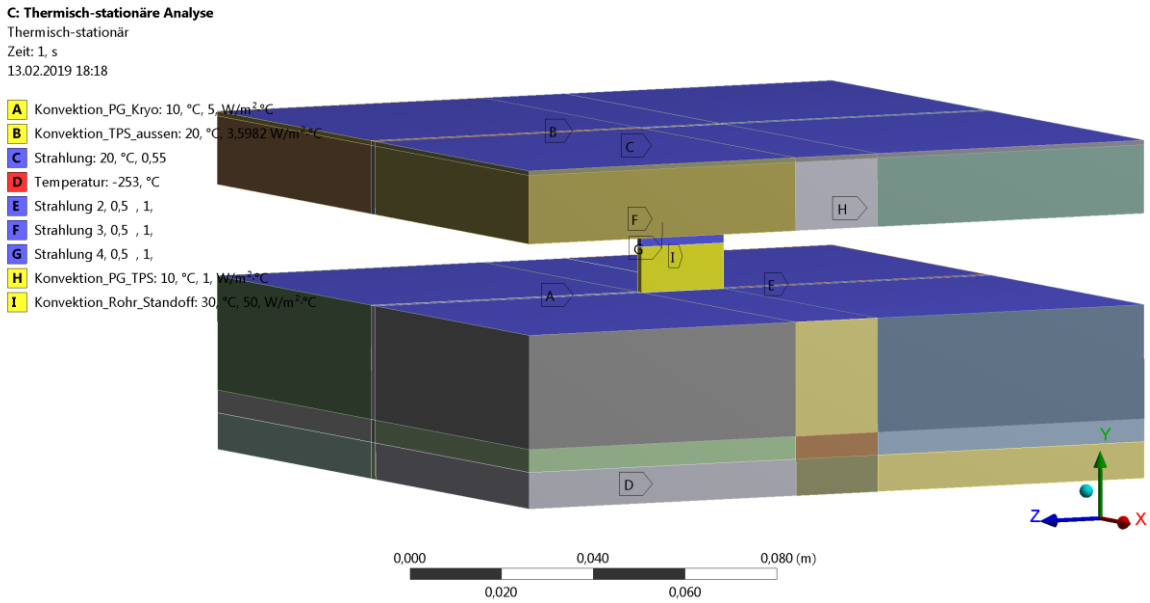

Figure 11: FE model for parametric investigation of fixation element materials and purge gap convection.

In Figure 12 the cross section through the model is shown along with the explanation of the individual geometric items which were used for parametric studies. It shows also the surfaces on which convection was applied.

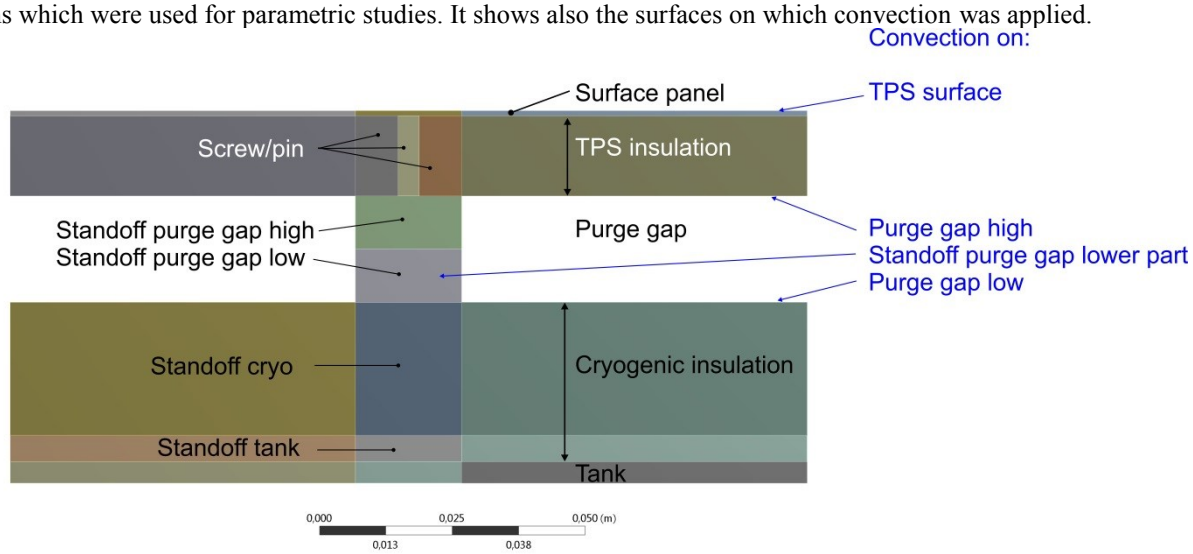

Figure 12: Elements of the structural connection between surface panel and tank.

The simulation methodology was to carry out a steady-state simulation of the temperature field representing the pre-launch situation and to check if the R1 requirement (temperatures in the TPS insulation over 0° C) was satisfied. Then that result was used as the starting condition for a transient simulation representing the ascent and re-entry of the vehicle after which it was checked if the R2 requirement was satisfied too (maximum temperature of the

DOI: 10.13009/EUCASS2019-345

cryogenic insulation 100° C). If either R1 or R2 was not satisfied, something was changed and the simulation started over. A first simulation, designation A, with materials as presented in Table 4 gave the result shown in Figure 13.

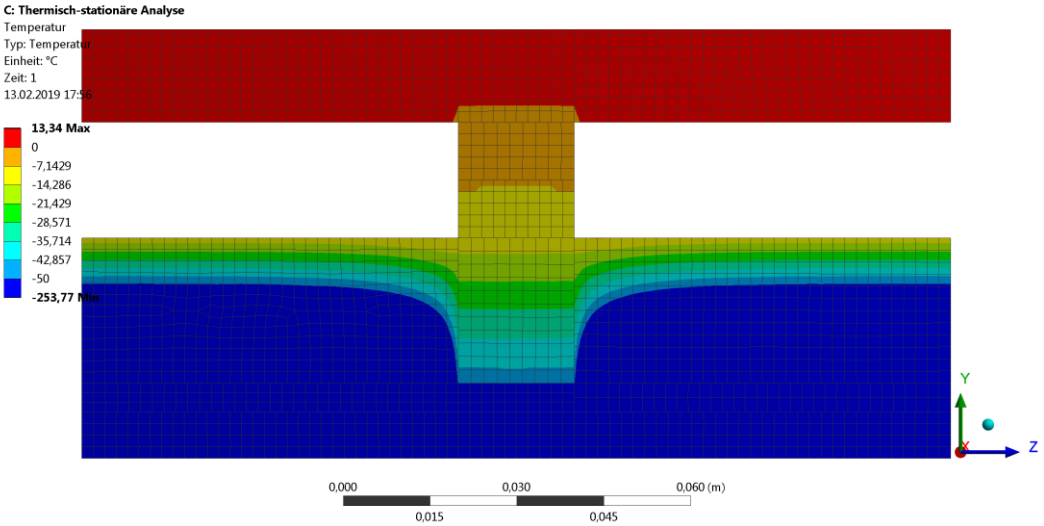

Figure 13: Steady-state condition first run.

It can be noted that in steady-state before launch, there is still some region of temperature lower than 0° C around the top of the standoff where it interfaces the TPS insulation, but this area is quite small and the requirement R1 is almost satisfied. In contrast to the steady-state solution, the temperatures during transient ascent and re-entry are way too high with this combination of materials and parameters. In Figure 14 the temperature plot at the time of the maximum surface temperature is shown, which is 781° C. The initial choice for the surface panel was titanium, but this temperature is too high for the material.

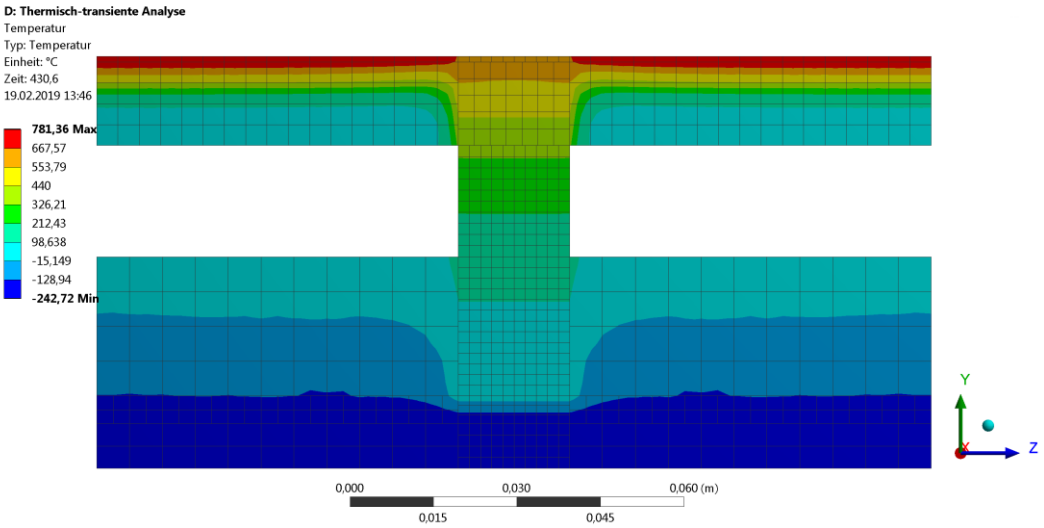

Figure 14: Maximum surface temperatures during re-entry.

Figure 15 shows the maximum temperature during re-entry for the cryogenic insulation. It occurs later than maximum surface temperature and is around 250° C. Also this is much too high for the Rohacell material. The material choice for the surface panel was changed to Inconel to lower the surface temperature. Inconel has a higher emissivity of up to 0.8 when it is pre-oxidised, compared to 0.55 for titanium. Several material options for the lower part of the standoff embedded in the cryogenic insulation were investigated, as there were CFRP, stainless steel 304 and also titanium. It turned out, that it is important to have an element of low thermal conductivity between tank and the lower part of the standoff to reduce the amount of convective heating required on the standoff in the purge gap region to keep the TPS insulation from going below zero degree Celsius. This element was finally selected as CFRP. Variations on the amount of convection applied on the standoff in the purge gap region were investigated. In Table 4 the values are given; they range from 50 to 150 W/m². Several combinations of materials and convection parameters

DOI: 10.13009/EUCASS2019-345

that satisfiy both requirements R1 and R2 were found and are listed as simulations D - F in Table 4. Convection in the purge gap was always 5W/m²K on the cryogenic side and 1W/m²K on the TPS side.

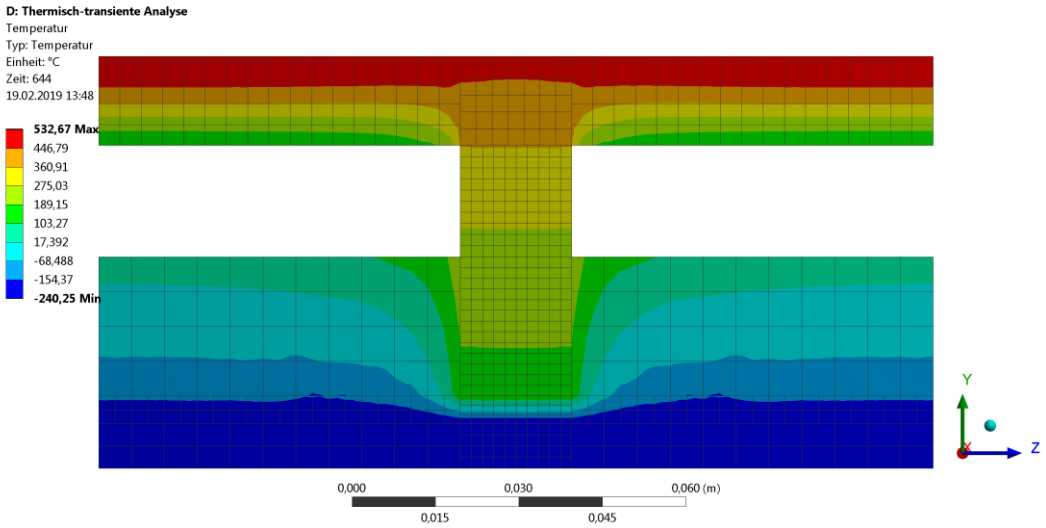

Figure 15: Maximum temperature of the cryogenic insulation during re-entry.

Table 4: Simulation parameters and temperature results for 3-D model of standoff and purge gap.

Sim. Run	Conv. SO	Mat. SO Tank	Mat. SO Cryo	Mat. SO PG low	Mat. SO PG high	Mat. Screw	Area screw	Mat. Panel	Temp. steady-state TPS-Ins.	max Temp. re-entry Cryo-Ins.	Max. surface Temp.
	W/m²K						mm²		°C	°C	°C
A	50	PK	Ti	SS	Ti	Ti	40	Ti	-1.4	**251.6**	**783.3**
B	110	CF	SS	SS	Ti	Ti	40	Ti	0.6	**180.4**	**783.3**
C	120	CF	SS	SS	Ti	In	40	In	0.3	**140.1**	640.0
D	150	CF	SS	SS	SS	In	8	In	1.6	-28.3	637.3
E	75	PK	SS	SS	SS	In	8	In	1.9	35.6	637.2
F	50	CF	CF	SS	SS	In	8	In	1.9	86.8	637.2
G	75	CF	SS	SS	SS	In	8	In	**-14.7**	-30.7	637.1

After simulation run C it was decided to change the cross section area of the screw element that attaches the panel to the standoff. In the first three runs it was set at 40 mm². However if a detailed design of a standoff is considered, this area is too high. It was then reduced to 8 mm² which is the equivalent of a cylinder with 3.2 mm diameter. This has a considerable effect on the temperatures. The area change together with an increased value for convection at the standoff brings temperature at the standoff/cryo-interface down to -28° C during the transient phase.

Two more variations were made from this point to see to which level the convection might be decreased without violating the requirements R1 and R2. The convection at the standoff was taken down to 75 W/m²K while changing the plate element under the foot of the standoff to Peek back again. In steady-state the temperature was still above 0° C and during the transient phase it went up to 35° C. The convection can be decreased further to 50 W/m²K if the conductivity of the lower element of the standoff is also reduced via choosing CFRP as its material. Doing so, the R1 requirement is kept with 1.9° C while the temperature of the Rohacell reaches 87° C during re-entry, which is still acceptable.

DOI: 10.13009/EUCASS2019-345

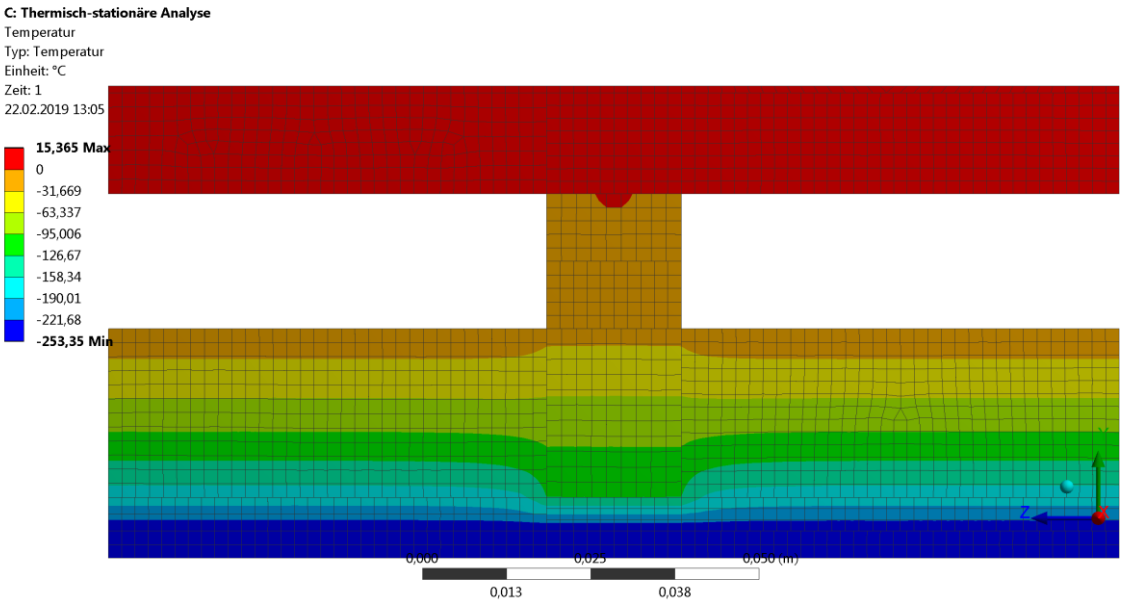

Figure 16: Simulation D steady-state results.

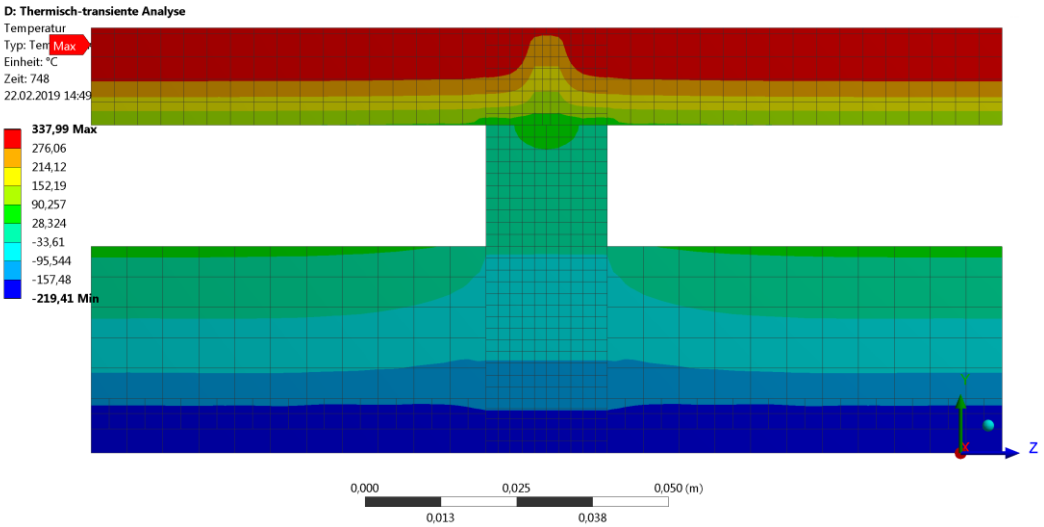

Figure 17: Simulation D transient result at time of maximum temperature on cryo-insulation.

Simulation G was done to see what happens if the convection at the standoff is reduced from 150 W/m²K to 75 W/m²K. This proves not to be feasible, the steady-state temperature at the TPS/standoff interface drops to -30° C.

6. Thermal Protection System Detailed Design

It was investigated how the standoff elements could actually be designed in detail based on the findings from the considerations and simulations shown. The overall dimensions used in the simulations were kept, i.e. a thickness of the cryogenic insulation of 30 mm, purge gap height of 20 mm, and a thickness of the TPS insulation of 15 mm.
A design suggestion was made which is shown in Figure 18. The connection between surface panel and the standoff is suggested to be made with just a pin, thereby relying on the elastic properties of the TPS insulation. An alternative solution with a threaded fastener is also possible, and in fact this will be realized for demonstration testing of the so-called Integrated Test Object (ITO). In addition, another variant was designed that incorporates a distance bushing between panel and standoff plus a wave spring to be independent from the stiffness of the TPS insulation. In that case, where there is just a pin, the upper element of the standoff is designed with a star pattern of slots which act as a receptacle for the pin tip.

DOI: 10.13009/EUCASS2019-345

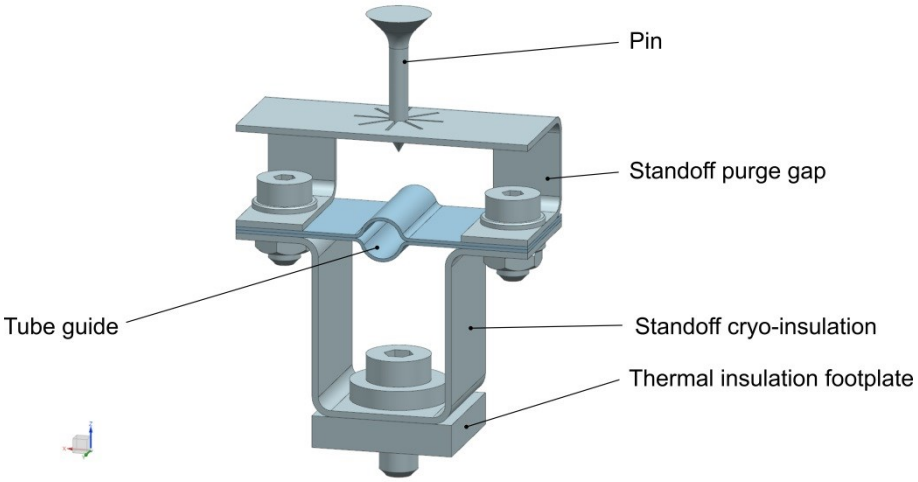

Figure 18: CAD model of standoff components.

In Figure 19 two cross-sections are given next to each other. The left-hand one features a C-profile in the region of the purge gap, making it mechanically flexible in the direction of the gas feedline-tube. The section on the right hand side shows an inverted hat profile which makes the standoff flexible in the direction perpendicular to the gas feedline-tube. This is an aspect that is considered because of the to be expected large thermal expansion effects with resulting mismatch between tank structure and surface panel.

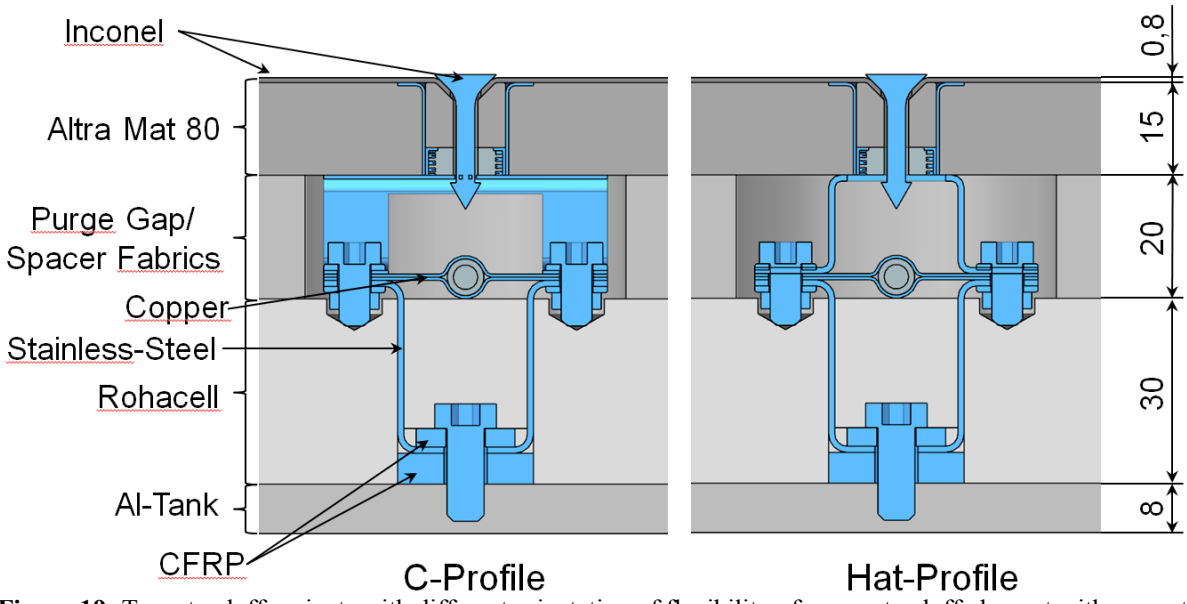

Figure 19: Two standoff variants with different orientation of flexibility of upper standoff element with respect to the tube direction. In both cases the variant with the bushing and spring is shown as well as dimensions.

7. AKIRA Project Integrated Test Object Definition

In the course of the AKIRA project, the proposed designs shall be realized as hardware and tested in a relevant environment to demonstrate the principal feasibility of the concepts and to validate the numerical models. The tests of the so-called ITO are to be conducted in different facilities of DLR according to the test objectives.
The main test objectives can be summarized as the following

- Cryogenic insulation properties
- Purge gap behaviour
- Thermal properties of the structural standoff assembly
- Standoff thermal control via the gas feed line

DOI: 10.13009/EUCASS2019-345

To this aim, three ITOs are being fabricated and tested. The test locations will be at DLR-Bremen, DLR-Cologne and DLR-Stuttgart. The focus of the tests in DLR-BRE will be on the low temperatures with a large ITO of approximately 1 x 1 m in size.
At DLR-KP the tests will be conducted in one of the LBK arc-heated wind tunnels to investigate the behavior of the model in a high-temperature plasma flow.
At DLR-ST the tests will be conducted on a medium-size ITO containing one standoff assembly plus the purge gap tubing including gas flow. The tests will be conducted in the induction-heated INDUTHERM facility of DLR. The ITO will be subjected to both the steady-state cooling as during pre-launch tank filling and as well to the subsequent high-temperature load as during re-entry. Steady-state cooling will be performed with active purge gap and liquid nitrogen representing the liquid fuel of the booster. Once the steady-state condition has been reached, liquid nitrogen re-filling is stopped so that it evaporates until the containment is empty. Then the test chamber will be closed, vacuum applied and the ascent and re-entry thermal cycle will be performed.
In order to facilitate the purge gap with the correct height of 20 mm, instead of designing and assembling some kind of auxiliary carrier structure from metal or composite, a flexible highly-porous spacer fabric is employed

8. Conclusions

To assess a possible insulation system design for a winged re-usable TSTO booster stage operating on cryogenic liquid fuel, investigations have been done on both the cryogenic insulation and as well on the TPS insulation with regard to their respective thickness and with regard to possible mechanical fixation of surface panels on the outside of the TPS.
A baseline configuration was looked at on the assumption that a dedicated cryogenic insulation is placed directly on the tank wall and then in turn the high-temperature insulation of the TPS is put directly on top of the cryogenic insulation. As criteria to assess the feasibility, two requirements were put up. First, the TPS insulation, being of a fibrous, open-cell type, should not go below the dew point of air to avoid condensation of moisture (we simplified that to 0° C); that was R1. Second, during the re-entry phase, the cryogenic temperature is limited to a maximum temperature of 100° C, that was R2.
Thermal analyses were done with this setup, using temperature-dependent material properties of the insulations. It turned out that the resulting overall thickness is on the order of 120 mm. That was seen as a critical issue because of two points. First, the large thickness is a considerable mass that has to be carried. Second, the analyses did not yet consider any realistic fixation elements going from the surface panels to the tank structure, which would certainly influence the temperature field.
As a result, the concept of a purge gap was investigated. Analytical calculations were done to assess the feasibility of the purging with regard to wall temperatures, geometry, amount of heat and gas velocity. The results showed that it should be possible to apply a purging system between cryogenic insulation and TPS insulation in order to thermally de-couple the two insulations from each other, resulting in a much reduced thickness of the cryogenic insulation.
The issue of local thermal disturbances introduced by the real-world standoff elements that connect tank and surface panels, was investigated via FE simulations. A 3-D model was developed, including the purge gap and a simplified standoff, to carry out parametric simulations with the aim to design the standoff in such a way that the two temperature requirements R1 and R2 could be satisfied. It was found that the standoff has to be designed from different parts with different materials, concerning their thermal conductivity, to arrive at a feasible design. In addition there has to be some convective heating of the standoff during the pre-launch phase to keep temperatures in the TPS from going too low.
Design solutions could be found for a configuration with 30 mm cryogenic insulation, 20 mm purge gap and 15 mm TPS insulation. A detailed pre-design of a possible standoff was presented, the individual elements being made from standard metallic materials.
Numerical simulations of the purge gap via CFD are ongoing to verify the analytical simulations and to prepare the upcoming demonstrator tests.
A test is prepared at different locations of DLR with a so-called ITO to verify the results of the design investigations. Specifically, at DLR-Stuttgart, the test will be set up in such a way that the whole cycle of the pre-launch cooling phase and the subsequent ascent and re-entry heat loads will be performed. The resulting data will then be used to validate the models and improve the design.
As an outlook to further work, it needs to be said that the booster considered here is just one possible reference vehicle respectively design. This specific booster design assumes the use of metallic aluminium tanks. In the case of a composite tank structure the picture will certainly change.
Moreover, the reference system is a TSTO vehicle, but only the booster was looked at for the moment. If the orbiter is investigated, this will for sure also require major changes to the proposed solutions since the trajectory with the related thermal loads is very different.

DOI: 10.13009/EUCASS2019-345

References

[1] M. Sippel, S. Stappert, J. Wilken, N. Darkow, S. Cain, S. Krause, T. Reimer, D. Stefaniak, M. Beerhorst, T. Thiele, R. Kronen, K. Schnepper, L. E. Briese, J. Riccius. Focused research on RLV-technologies : the DLR project AKIRA. EUCASS 2019, July 01-04, Madrid, Spain

[2] M. Sippel, O. Trivailo, L. Bussler, S. Lipp, C. Valluchi. Evolution of the SpaeLiner towards a Reusable TSTO-Launcher, IAC-16-D2.4.03

[3] VDI-Wärmeatlas; Verein Deutscher Ingenieure VDI-Gesellschaft Verfahrenstechnik und Chemieingenieurwese (GVC); Springer, 10. Auflage, 2006, Heidelberg

[4] M. L. Blosser, R. R. Chen, I. H. Schmidt, J. T. Dorsey, C. C. Poteet, R. K. Bird, K. E. Wurster. Development of Advanced Metallic Thermal –Protection-System Prototype Hardware. J. of Spacecraft and Rockets, Vol. 41, No. 2, Mar-Apr 2004